Strength assessment of Al-Humic and Al-Kaolin aggregates by intrusive and non-intrusive methods

Moruzzi, Rodrigo; da Silva, Pedro Grava; Sharifi, Soroosh; Campos, Luiza C.; Gregory, John

DOI:
10.1016/j.seppur.2019.02.033

STRENGTH ASSESMENT OF AL-HUMIC AND AL-KAOLIN AGGREGATES BY INTRUSIVE AND NON-INTRUSIVE METHODS

Rodrigo B. Moruzzi[a*], Pedro Grava da Silva[b], Soroosh Sharifi[c], Luiza C. Campos[d], John Gregory[d]

[a] Instituto de Geociências e Ciências Exatas, Univ. Estadual Paulista (UNESP), Av. 24-A, 1515, Jardim Bela Vista, Rio Claro, 13506-900. São Paulo, Brazil. E-mail: rmoruzzi@rc.unesp.br

[b] Programa de Pós-graduação em Engenharia Civil e Ambiental, Univ. Estadual Paulista (UNESP), Av. 24-A, 1515, Jardim Bela Vista, Rio Claro, 13506-900. São Paulo, Brazil. E-mail: pedroagrava@gmail.com

[c] Department of Civil Engineering, University of Birmingham, B15 2TT, United Kingdom. Email: S.Sharifi@bham.ac.uk

[d] Department of Civil, Environmental and Geomatic Engineering, University College London, Gower St, London, WC1E 6BT, United Kingdom. E-mail: l.campos@ucl.ac.uk

Address:

* Corresponding author: Avenida 24-A, nº 1515, C. P. 178, CEP 13506-900, Office 23, Bela Vista, Rio Claro, São Paulo, Brazil. Phone: +55 19 3526-9339. *E-mail address*: rmoruzzi@rc.unesp.br

Abstract:

Resistance to breakage is a critical property of aggregates generated in water and wastewater treatment processes. After flocculation, aggregates should ideally keep their physical characteristics (i.e. size and morphology), to result in the best performance possible by individual separation processes. The integrity of aggregates after flocculation depends upon their capacity to resist shear forces while transported through canals, passages, apertures, orifices and other hydraulic units. In this study, the strength of Al-Humic and Al-Kaolin aggregates was investigated using two macroscopic measurement techniques, based on both intrusive and non-intrusive methods, using image analysis and light scattering based equipment. Each technique generates different information which was used for obtaining three floc strength indicators, namely, strength factor (*SF*), local stress from the hydrodynamic disturbance (σ) and the force coefficient (γ) for two different study waters. The results showed an increasing trend for the *SF* of both Al-Humic and Al-Kaolin aggregates, ranging from 29.7% to 78.6% and from 33.3% to 85.2%, respectively, in response to the increase of applied shear forces during flocculation (from 20 to 120 s^{-1}). This indicates that aggregates formed at higher shear rates are more resistant to breakage than those formed at lower rates. In these conditions, σ values were observed to range from 0.07 to 0.44 N/m² and from 0.08 to 0.47 N/m² for Al-Humic and Al-Kaolin, respectively. Additionally, it was found that for all studied conditions, the resistance of aggregates to shear forces was nearly the same for Al-Humic and Al-Kaolin aggregates, formed from destabilized particles using sweep coagulation. These results suggest that aggregate strength may be mainly controlled by the coagulant, emphasizing the importance of the coagulant selection in water treatment. In addition, the use of both intrusive and non-intrusive techniques helped to confirm and expand previous experiments recently reported in literature.

Keywords: Aggregates, floc resistance, image analysis, flocculation.

1. Introduction

Most solid-liquid separation processes work by increasing the size of the particulate matter, leading to the formation of aggregates or flocs. The performance of solids removal is dependent on the physical characteristics of the aggregates that need to be compatible with the separation method used (Yukselen and Gregory, 2004). Among these characteristics, the floc strength, which is an expression of resistance to breakage, is crucial for effective particle separation in clarification units, such as sedimentation tanks, dissolved air flotation units and membrane filtration (Jarvis *et al.*,2005).

It is well-documented that, solid-liquid processes are negatively affected by the breakage of flocs, as only limited regrowth of broken flocs can occur, thus leading to low removal efficiency in sedimentation units (Yukselen and Gregory, 2002, 2004; Yu *et al.*, 2010b, 2011, 2015). The floc strength is also linked to problems in treatment plants with rapid sand filtration, in which the small resistance of the aggregates to the hydrodynamic variations has a damaging impact on the filter media, shortening their operational life and resulting in pollutant trespassing (Moruzzi and Silva, 2018). Therefore, water treatment plants should ideally be designed to minimize floc breakage; however, despite the recommendations, it is difficult to precisely determine how much stress a previously formed floc can take without breaking.

When the shear rate is larger than floc strength, the flocs either break into approximately equal size fragments, or under some circumstances, erosion of small particles from the flocs' surface may occur. In turbulent flow, the breakage type depends on the size of the flocs in relation to the micro-scale of turbulence (Mühle, 1993). Because of floc breakage, some regions of the floc surface may become inactive and incapable of forming new bonds of attachment to other flocs, thus reducing the flocculation efficiency (Yu *et al.*, 2011). The fact that broken flocs do not fully regrow when the original low shear rate is restored means that the binding between particles is weaker (Yu *et al.*, 2010b).

It is well acknowledged that the floc strength is dependent on the bonds between aggregate component particles (Parker *et al.*, 1972, Bache *et al.*, 1997). This includes the strength and number of individual bonds within the floc. However, recent studies (e.g. Yu *et al.*, 2015) have shown that kaolin particles incorporated within hydroxide flocs appear to have no influence on floc properties, including floc strength and size. Younker and Walsh (2016) demonstrated that the

addition of adsorbents to metallic salt flocs did not increase or reduce floc strength. Conversely, kaolin flocs formed by ferric coagulants were found to be larger and stronger than those formed by alum coagulants (Zhong *et al.*, 2011). Bridging flocculation by long-chain polymers can generate very resistant flocs, while the destabilization of particles by low dosages of inorganic salts results in fairly weak flocs (Yukselen and Gregory, 2004; Wang *et al.*, 2009; Yu *et al.*, 2015).

Humic acids have been widely used as natural organic matter to investigate floc properties after flocculation. It has been shown that humic flocs growth is not determined by the flocs' size distribution (Yu *et al.*, 2010b, 2012), but by some of their properties, including floc strength, which is mostly dependent on the surface activity of flocs, and coagulant species formed from Alum and Iron hydrolysis (Wang *et al.*, 2009).

Moruzzi and Silva (2018) carried out experiments on Al-Humic and Al-Kaolin aggregates and showed that flocs formed from sweep coagulation mechanism, by different particulate matter and the same coagulant have similar regrowth patterns, indicating similar binding between particles for Al-Humic and Al-Kaolin, as presented by Yu *et al.* (2010b). On the basis of these findings, it is speculated that Al-Humic flocs strength might have similar resistance to shear forces as Al-Kaolin flocs. In this case, the resistance of the flocs to shear rate could be attributed to the used coagulant, corroborating with results presented by Yu *et al*. (2015).

For determining aggregate proprieties, such as size and floc strength, monitoring techniques should be applied during flocculation. Intrusive techniques, such as those based on light scattering, have been conventionally used for monitoring aggregates during flocculation (Yukselen and Gregory, 2002; 2004; Yu *et al.*, 2011). However, these techniques require taking frequent samples from the water into measurements chambers, a process that may cause some damage to aggregates due to their fragile nature. In some cases, flocs damage may be minimized by limiting the average gradient velocity during the sample extraction, controlling inner tube size and flow through tube, as presented by Gregory (1981) and Yu *et al.* (2010b). Recently, however, flocculation monitoring by non-intrusive image analysis has shown promising results (Li *et al.*, 2007; Moruzzi *et al.*, 2017; Moruzzi and Silva, 2018) and has allowed the determination of floc strength, among other floc characteristics.

In practice, the strength of the floc is often determined in an empirical way, usually by establishing a relationship between the floc size and the applied shear rate (François, 1987; Jarvis *et al.*, 2005, Li *et al.*, 2007). This empirical approach was firstly suggested by Parker *et al.* (1972), and it has been used extensively in theoretical and experimental research to evaluate maximum floc size under a given turbulent intensity (e.g. Bache, 1989; 2004 and Li *et al.,* 2006; 2007).

There are two fundamental approaches to measuring the strength of the floc *i.e.* a macroscopic approach, which measures the system energy required for breakage of flocs, and a microscopic approach, which measures the interparticle forces within individual flocs (Jarvis *et al.*, 2005). In the microscopic approach, the strength can be measured by applying a shear stress or a normal stress to a floc individually. On the other hand, macroscopic techniques preform an indirect evaluation of the floc resistance by means of analysing the energy dissipation, or the mean velocity gradient (G), applied to maximum- or average-sized flocs. This approach originated from the empirical relationship between the applied hydrodynamic shear rate and the resulted floc size (Jarvis *et al.*, 2005).

This work aims to investigate the floc strength for both Al-Kaolin and Al-Humic aggregates by means of macroscopic indicators, and to demonstrate the insignificant effect of the particulate matter within the flocs on their properties, namely size and strength. For the first time, image analysis is applied concomitantly with photometric dispersion to obtain the strength factor (SF), local stress from the hydrodynamic disturbance (σ) and the force coefficient (γ). The combined application permits the comparison and establishment of correlations between the data obtained from two different techniques (intrusive and non-intrusive). This is the first time image and photometric dispersion of Al-Humic acid flocs is measured by this technique and the results from the two complementary methods is used to understand the factors affecting floc strength.

2. Materials and Methods

2.1 Study Waters

Two water samples were prepared from stock suspension of kaolin and from stock solution of humic acid. For sample one, hereafter referred to as type 1, a humic acid solution prepared from lyophilised natural organic matter (*Aldrich Chemical*) with concentration of 30 mg/L was used to obtain 50 units of Platinum-Cobalt Scale - PtCo at 455 nm, as the initial condition (Moruzzi and

147 Silva, 2018). For the second sample (type 2), a kaolin suspension was prepared from a
148 commercial kaolin (Sigma-Aldrich) to obtain 25 units of turbidity scale as Nephelometric
149 Turbidity Units - NTU (Moruzzi *et. al*, 2017 and Yukselen and Gregory, 2004).

150 Coagulation was performed by dosing alum [$Al_2(SO_4)_3 \cdot 18H_2O$] using sweep-coagulation
151 mechanism, following recommendations by Oliveira *et al.* (2015). So, dosages of 10 and 30
152 mgAl^{+3}/l at pH of 7.5 and 4.5 were applied for Al-Kaolin and Al-Humic aggregates formation,
153 respectively. Sodium hydroxide (NaOH) 1 mM was used as a buffer during coagulation to control
154 pH. All tests were performed at room temperature (20 ± 2 °C).

155 *2.2 Flocculation and strength tests*

156 Jar tests were performed for flocculation and breakage experiments (*Ethik Technology Model*
157 *218/6 LDB*). The method applied consists of an intrusive and non-intrusive image-based
158 acquisition method and photometric dispersion analyser (PDA), similar to that used by Yu *et al.*
159 (2015). Here, however, both image and photometric dispersion were applied at the same time to
160 obtain strength indices, thus permitting comparison and correlation of results. A simplified
161 schematic of the experimental apparatus, including Jar Test, the image-based system and light-
162 scattering monitoring equipment, is shown in Figure 1.

163 A mean velocity gradient of 800 s^{-1} was applied for 10 seconds to ensure a rapid mixing, and also
164 for flocs breakage in all light scattering tests, based on preliminary tests (Oliveira *et al.*, 2015).
165 This standard shear rate was chosen for taking a central position in the typical shear range of
166 predominant erosion breakage as proposed by Mikkelsen and Keiding (2002), and the duration
167 was sufficient for the coagulant transportation (Yukselen and Gregory, 2004). For flocculation,
168 the following velocity gradients (G) were applied: 20, 30, 40, 50, 60, 80, 100 and 120 s^{-1}. For the
169 trials involving PDA measurements, G values were kept constant during the first 25 minutes, and
170 after this period, G was set to 800 s^{-1} for 10 seconds to induce breakage of flocs. This short period
171 of time was chosen to simulate the water passage in gates and orifices that normally occur after
172 flocculation.

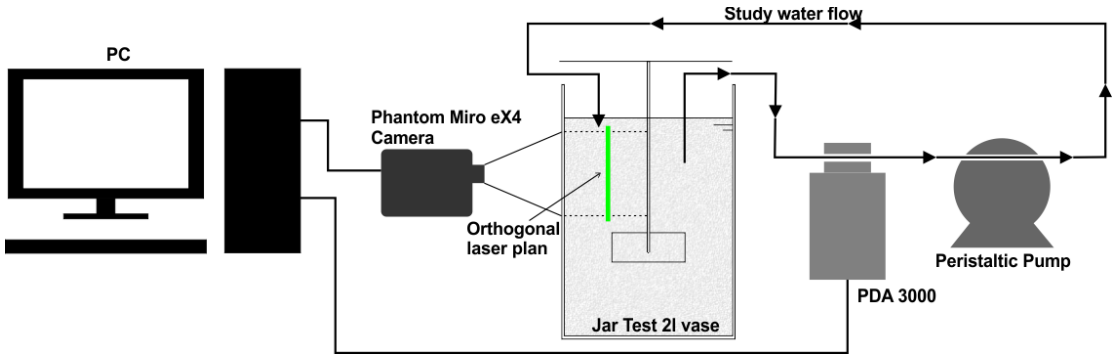

Figure 1. A simplified schematic of the experimental apparatus.

2.3 Image Analysis

The image analysis applied here was strictly used to obtain aggregates size, which in turn was used for floc strength indicator calculations, namely local stress from the hydrodynamic disturbance (σ) and the force coefficient (γ), as presented in Section 2.6. Images were captured in 2^8 bit monochromatic mode (*i.e.* 256 grey scale) using a *Vision Research Miro EX4* camera together with a set of lenses, and 840 pixel x 640 pixel of image resolution, to obtain a pixel size of 10 μm. A laser sheet of 20,000 mW and wavelength of 520 nm provided the lighting as described by Oliveira *et al.* (2015) and Moruzzi *et al.* (2017).

Samples were obtained at 5-minute intervals (from 5 to 25 minutes) to assess floc size at a given flocculation time (T) of interest, *i.e.* those usually applied in drinking water treatment plants. Each image package was taken over a short duration of 10 seconds with a frequency of 10 Hz (Figure 2-a) to precisely describe the system situation at that given time of interest. This sample time and frequency was sufficient to capture a reliable picture of the floc characteristics at the required flocculation time along with a statically representative number of flocs within the 10 seconds sampling time.

The image processing software *Image-Pro-Plus*® (IPP) was used to develop the images, *i.e.* conversion from 2^8 to 2^1 bits, enhancement and measurement (Figures 2-b to 2-d). Only aggregate sizes longer than 100 μm (≥10 pixels) were monitored for image precision, as recommended by Chakraborti *et al.* (2003).

In total, 197,207 aggregates were measured from 7,200 frames (average of 27 aggregates/frame) for Al-Humic water, and 141,609 aggregates were measured from 6,800 frames (average of 21

aggregates/frame) for Al-Kaolin water. In these sample sizes, floc size errors were lower than 4.0% and 4.6% at 95% of confidence interval for an infinite population of Al-Humic and Al-Kaolin aggregates, respectively. Figure 2 illustrates the different steps involved in the image processing procedure applied here, from acquisition to image processing and size measurement.

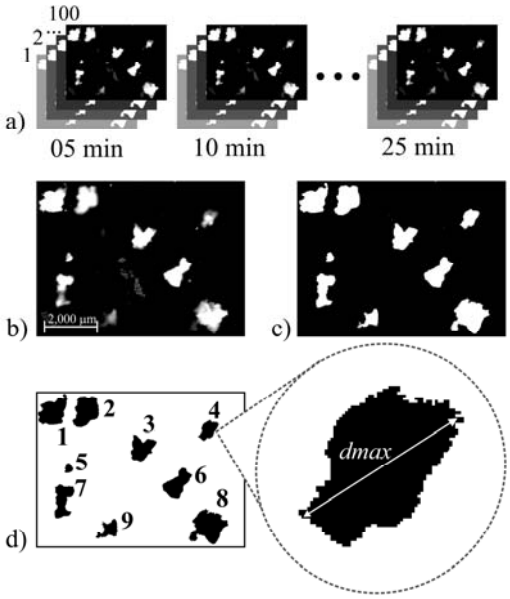

Figure 2. An example of image conversion enhancement and measurement: (a) Image acquisition using on 10 Hz during 10 seconds for each flocculation time (T), resulting in a pack of 100 frames per G *x* T; (b) Flocs in grey scale (2^8 bits); (c) Image after threshold with black and white pixels only (2^1 bits); (d) Counting and measuring flocs by IPP 7.0 software®.

2.4 Light Scattering

The light scattering approach applied was strictly used to obtain the flocculation index (*FI*), which will be better explained in the following sections. Light scattering analysis was performed using a *Photometric Dispersion Analyser* (PDA), and the obtained results were used for calculating the strength factor, which will be introduced and presented in Section 2.6. In PDA equipment, samples flow through a 3-mm-diameter tube where the intensity of a narrow beam of light is monitored by a sensitive photodetector following Yukselen and Gregory (2004) and Moruzzi *et al.* (2017). Although intrusive technologies can cause some damage to flocs, in PDA this can be minimised by controlling the average gradient velocity during sample extraction. Here, the flow rate through the sampling tube was controlled to enforce laminar flow regime

(Reynolds number ≤ 80) and shear rates lower than 50 s^{-1}, as shown by Gregory (1981); conditions where damage is considered insignificant, as also shown by Yu *et al.*, 2010b. Further, the water samples were circulated by means of a peristaltic pump located after the PDA instrument to avoid the effects of possible floc breakage in the pinch part of the pump (Figure 1), as performed by Li *et al.* (2007).

The *PDA 3000* measures the average transmitted light intensity (dc value) and the root mean square (rms) value of the fluctuating component. The ratio (rms/dc) provides a measure of the balance of particle aggregation (Gregory, 1984; Gregory and Nelson, 1986; Yukselen and Gregory, 2004; Yu *et al.*, 2010b), hereafter referred to as flocculation index (*FI*). Up to a limited size, the *FI* value is strongly correlated with floc size and always increases as flocs grow larger, but the *FI* value can become uncertain when flocs are larger than 250 μm and absolute floc size cannot be taken from *FI* signals (Yu *et al.*, 2010a; Yu *et al.*, 2010b and 2011). Also, larger aggregates have a predominant influence on the ratio value (Gregory, 1984), thus affecting *FI* signals. Therefore, the PDA shows qualitative changes in flocs, as reported by Gregory and Nelson (1986), but the instrument is unable to give an absolute particle size. Further, the *FI* signals vary with both particle size and particle number and it is not possible to know the precise contribution of each of these components in the *FI* signal. Yu *et al.* (2015) have shown that flocs with similar size can have very different *FI* values, confirming the idea that *FI* does not give an absolute indication of size for hydroxide flocs. However, the generated signal can be used as an indicator of aggregation, as shown by Gregory (1985), and also as a measure of floc strength as shown by Li *et al.* (2007), Gregory (2009) and Yu *et al.* (2010b). More details are given in the following sections.

2.5 Floc size and FI determination

The macroscopic techniques used for the study of the floc strength were developed based on the relationship between the applied hydrodynamic shear rate and the resulting floc size. According to Gregory (2003), floc size and *FI* can be both used as floc strength indicators for a given shear rate. In order to obtain the floc strength indicators, which are related directly to the size limit reached by the floc, two different sources of information were utilized: one from the image analysis and another from the PDA.

For image analysis, the average diameter (d) of aggregates was determined from the average of the longest length of the aggregates (d_{max}) in the selected times of interest, following Li *et al.* (2007):

$$d = \frac{1}{n}\sum_{i=1}^{n} d_{imax} \qquad (1)$$

where d is the average of d_{max} (μm), d_{max} is the longest length (μm), as shown in Figure 2, and n is the number of counted aggregates in a sample varying from i = 1, 2 …, n.

The d values obtained from Equation 1 represents the average of d_{max}, measured for each one of the eight investigated flocculation times (T), *i.e.* 5, 10, 15, 20, 25, 30, 35 or 40 minutes. It is important to emphasize that, flocculation kinetics were not the focus of this paper, but rather the floc strength assessment at given flocculation times of interest, where the dynamic equilibrium between flocs breakage and aggregation could be indirectly observed by the floc size. Therefore, the d value represents the balance between flocs aggregation and breakage at a given time of flocculation, and its average size tends to a stable value, *i.e.* a limiting size, for a given shear rate as the steady state regime is reached. When little variation is observed in floc size, the average size of d remains oscillating slightly around a maximum value, which is referred to as the plateau.

The plateau was determined from the incremental variation of the average diameter (d) during flocculation. This variation tends to a narrow range because of the dynamic steady state. The incremental variation can be determined by:

$$\Delta d_i = \left|\frac{(d_i - d_{i-1})}{d_i}\right| \qquad (2)$$

where Δd_i is the incremental variation of average diameter between the time interval t_i-t_{i-1}, with i = 1,2, ..., n.

The typical value of the diameter in the plateau was then determined from the average of diameters within $\Delta d \leq 10\%$. Hypothesis tests were also performed to confirm the plateau with significance of 0.05.

The analysis based on light scattering was done through the *FI* signal generated from the PDA. The maximum value observed in the stationary flocculation phase was adopted once the plateau

was reached at that time interval. For FI_2, the value adopted was the minimum point at the instant of the induced rupture, following Li *et al.* (2007). Here, the rupture shear rate of 800 s^{-1} was applied for 10 seconds, at the flocculation time of 25 minutes. Figure 3 schematically shows how FI_1 and FI_2 are determined from the *FI* signal.

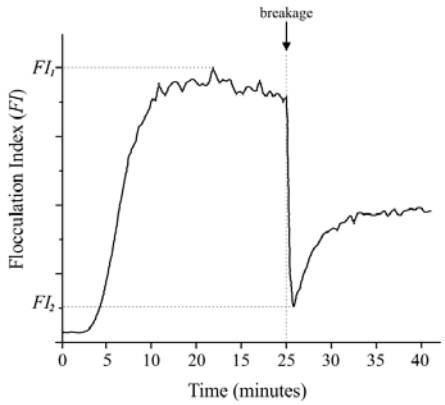

Figure 3. Schematic representation of the *FI* signal, with indication of the values of FI_1, FI_2 and induced breakage by applying velocity gradient of 800 s^{-1} at 25 minutes (adapted from Li *et al.*, 2007).

2.6 Floc strength indicators

As mentioned in previous sections, the floc strength indicators presented here were determined using both image analysis and PDA. For the image analysis method, *d* values were taken, whilst for PDA only *FI* signals were used.

Floc strength coefficient (γ)

The floc strength coefficient (γ) was obtained from image analysis using Equation 3 that describes the stable size determined from image analysis as a function of the mean velocity gradient applied to the system during flocculation, firstly suggested by Parker *et al.* (1972):

$$d = C \cdot G^{-\gamma} \qquad (3)$$

where C is the multiplicative constant (μm/s), G is the average velocity gradient (s^{-1}), and γ is the floc strength coefficient (dimensionless), obtained from stable floc size.

The floc strength coefficient (γ) can be calculated using mean, median and longest length of flocs with nearly the same results, as reported by Leentvaar and Rebhun (1983). For the results

295 presented here, d values were calculated using the longest length of flocs obtained during
296 flocculation from different shear rates according to Equation 1.

297 The *ln-ln* plot of Equation 3 against the average gradient velocity applied during flocculation
298 results in a line, which its slope is indicative of floc strength. The inverse relationship of
299 proportionality indicates that the higher the value of γ, the more prone the floc is to breakage
300 under increasing shear rates, resulting in smaller aggregates (Li *et al.*, 2007). Therefore, the value
301 of γ is considered as an indicator of its strength. This concept was proposed by Parker *et al.*
302 (1972) and is adopted in the study of Li *et al.* (2007). Here, the floc strength coefficient (γ) was
303 determined from the slope of linear best fit to the *ln-ln* plot of Equation 3, using experimental
304 data for the study waters. It is worth noting that the value of C can also be used as a floc strength
305 indicator, but only within the same experimental conditions, as its value depends upon the
306 method used for particle size measurements and the choice of the characteristic value of d (Jarvis
307 *et al.*, 2005).

308 *Strength factor (SF)*
309 The strength factor (*SF*) has been previously used by several researchers (*e.g.* Li *et al.*, 2007; Yu
310 *et al.,* 2010b and 2015; Su *et al.,* 2017) to compare the breakage and the strength of flocs in
311 different shear rate conditions for Al-Kaolin aggregates. The results of these studies indicate that
312 this parameter can be effectively used as a floc strength index. *SF* is calculated based on *FI*
313 signals only and used to characterize the aggregate size maintenance capacity, following
314 Yukselen and Gregory (2002):

315 $$SF\ (\%) = \frac{FI_2}{FI_1} 100 \qquad (4)$$

316 where FI_1 is the maximum *FI* value before breakage, and FI_2 is the *FI* value right after the
317 breakage period, as shown in Figure 3. In this study, FI_1 was calculated from different shear rates
318 and FI_2 was always determined after applying a shear rate of 800 s^{-1}, as described in Section 2.5.

319 High values of the *SF* indicate that flocs are better able to withstand shear rates, and therefore, the
320 higher the value of *SF*, the stronger the flocs can be considered for a given rupture shear rate
321 (Jarvis *et al.*, 2005). It is important to note that *SF* is not constant, the shear rate applied during

the breakage strongly affects FI_2 (Yu *et al.*, 2010b), and so, *SF* can only be compared for similar induced rupture conditions. Here, the average velocity gradient of 800 s^{-1} was applied for rupture.

Hydrodynamic disturbance (σ)

In addition to the above-mentioned empirical methods for obtaining a force coefficient, Bache *et al.* (1997) proposed a theoretical method where the mean force applied per unit area of the system, σ (N/m^2), could be determined by:

$$\sigma = \frac{4\sqrt{3}}{3}\frac{\rho_w \varepsilon^{3/4} d}{\nu^{1/4}} \qquad (5)$$

where ρ_w is the density of the water (kg/m^3), $\mathcal{E}$ is the local energy dissipation rate per unit mass (m^2/s^3), d is the average of the longest length of aggregates at a given time, measured by image analysis (m) and ν is the kinematic viscosity (m^2/s) at room temperature of 20 ± 2°C.

Parameter $\mathcal{E}$ is usually replaced by $\bar{\mathcal{E}}$ (Equation 6), which is the average rate of dissipation of the local energy per unit mass and is directly proportional to *G*, a parameter easily administered during the experiment:

$$\bar{\mathcal{E}} = \nu G^2 \qquad (6)$$

where ν is the kinematic viscosity (m^2/s).

3. Results and Discussion

3.1 Image analysis

Figure 4, as an example, presents the time evolution of d and Δd obtained from Equations 1 and 2, respectively, for various velocity gradients (G) applied to study water type 2. For d evolution (Figure 4-a), aggregates have grown for time intervals between 5 and 10 minutes and for G from 20 to 40 s^{-1}. After 10 minutes of flocculation, only G of 20 s^{-1} has resulted in aggregates increment for d. Consequently, the incremental variation of floc size (Figure 4-b) is observed to be smaller than 10% for the majority of the analysed velocity gradients during the flocculation at times 10-15 and 15- 20 minutes (except for G of 20, 30 and 40 s^{-1}), indicating the establishment of steady-state conditions. Thus, d was obtained by averaging d during the period 15-20 minutes, when significant stability was observed, *i.e.* when the stable size of d was reached. For these time intervals, test of hypothesis has shown that there is no significant difference between the two

water types for p-value of 0.05, *i.e.* for both Al-Humic and Al-Kaolin the average diameter did not change for time intervals from 15 to 20 minutes, making it possible to confirm the plateau.

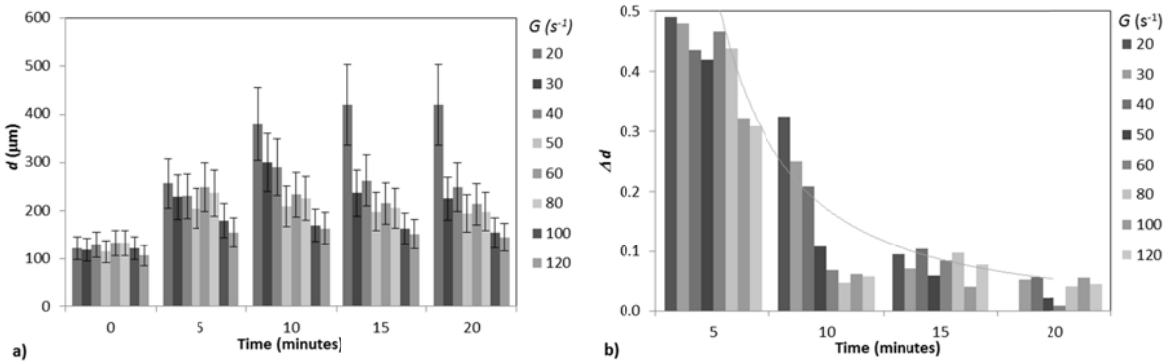

Figure 4. Time evolution of (a) *d* and (b) *Δd* during flocculation time (for discrete intervals of 5, 10, 15 and 20 minutes) for water type 2. Fluctuation bars in (a), represent standard derivations and the decay curve in (b), represents the overall trend of *Δd* during time. Time zero in Fig. 4-a shows flocs size measurements in the very beginning of flocculation and those results were used as d_{i-1} for *Δd* calculation in time of 5 minutes, as Equation 2.

Figure 5 shows the relationship between *ln* (*d*), calculated by Equation 1, and *ln* (*G*), where the slope of the trend line, as described by Equation 3, indicates the floc strength coefficient *γ*, Once *γ* value remains constant, any variant characteristic of *d* (*i.e.* mean, median or maximum length) can be used for comparing results among different studies (Jarvis *et al.*, 2005). A decreasing tendency of the stable size *d* in response to the increase of *G* was observed at a rate near 0.45 for the two study waters, which is in the range of 0.44 to 0.63 reported by other researchers (*e.g.* Bache and Rasool, 2001; Francois, 1987; Li *et al.*, 2007) when using alum as coagulant for Al-Humic and Al-Kaolin flocs.

The obtained *γ* value for the two study waters indicates that Al-Humic and Al-Kaolin flocs are similarly able to resist shear rates, as the steepness of the *ln-ln* plot slopes are nearly the same for both waters (0.45). The analysis of *C* from Equation 3 is not commonly used for floc strength evaluation, as it depends upon which characteristic of *d* has been used, and wide variation between different studies has been reported, *e.g.* from *ln C* of 7.1 to 9.4 according to Bache *et al.* (1999) and Bache and Rasool (2001), respectively. However, *C* can be also used to compare floc strength within specific experimental system (Jarvis *et al.*, 2005). Results presented here have shown *C* values of 1305 (*ln C* of 7.17) and of 1399 (*ln C* of 7.24) for Al-Humic and Al-Kaolin,

respectively, thus reinforcing that Al-Humic and Al-Kaolin have nearly the same ability to resist applied shear forces. These results are in agreement with the finding by Yu *et al.* (2015) who found that the nature of primary particles has no influence on floc strength when sweep coagulation mechanism is applied and once flocs rapidly grow and incorporate most particles within the hydroxide precipitate. Also, the use of a non-intrusive technique, such as the image analysis system here applied, permits to confirm the previous findings by Yu *et al.* (2015), once it is not influenced by possible interferences caused by samples extraction and light scattering, as presented by Gregory (2009) and Yu *et al.* (2015).

The analysis of strength coefficient (γ) can also be related to turbulent shear patterns due to eddy size, as proposed by Biggs and Lant (2000) and Bache (2004), resulting in different floc breakage modes during flocculation. Based on the analysis of the dominant mode of floc degradation presented by Parker (1972) and François (1987), the results presented here for γ (Figure 5) indicate that the flocs are more prone to breakage due to a dominant effect of fragmentation, as the result of the viscous energy dissipation, once the floc strength coefficient γ was around the theoretical value of 0.5. This is an indication that small eddies (*i.e.* the turbulence micro-scale) is of a similar order of magnitude to the flocs sizes (Mühle, 1993; Jarvis *et al.*, 2005). However, fragmentation and erosion are expected to occur at the same time, as large flocs in an aggregated system may be larger than the micro-scale whist smaller flocs may be smaller than micro-scale (Biggs and Lant, 2000).

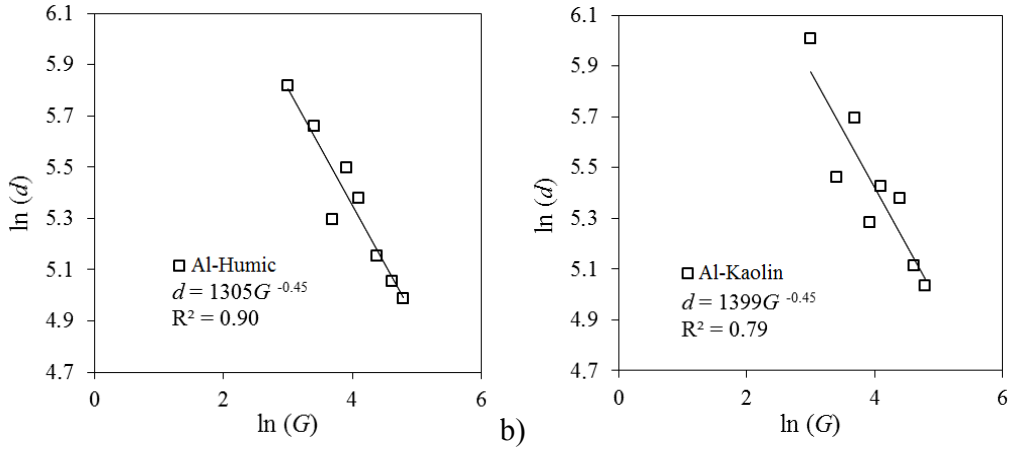

Figure 5. Relationship between *ln d versus ln G* during flocculation: (a) water type 1 – Al-Humic and (b) water type 2 – Al-Kaolin. *ln d* was obtained by averaging *d* during the period 15-20 minutes, where $\Delta d < 10\%$ was observed.

3.2 Light scattering

Figure 6 shows the temporal evolution of the *FI* signal (obtained by PDA) in the tests carried out. It is clearly observed that in the flocculation [0-20 minutes] and regrowth [25-40 minutes] phases, the floc size tend towards a stabilized plateau. The sharp drop of *FI* at 25 minutes was the point where the induced breakage occurred. The difference in the signal scale between the two study waters is caused by the different light scattering properties, *e.g.* floc density and scattering cross-section, which are also dependent on both particle concentration (in terms of volume, mostly) and type (Gregory, 2009). This difference has important implications for the monitoring of floc size by light scattering methods as also observed by Yu *et al.* (2015). Similar fluctuation on *FI* values were observed by Gregory (2009), while studying optical proprieties of flocs using PDA for different waters. The author concluded that scattering cross-section is expected to be different when different concentration of impurities, as clay, are within flocs and so *FI* signals vary. However, the results obtained by Gregory (2009) have shown that curves are rather similar in shape, showing the same relative increase in *FI* during floc formation. Therefore, although scattering proprieties can limit direct comparisons of *FI* values among different waters, it is not expected to affect the strength factor (*SF*) given by Equation 4, once it is determined as a ratio for the same water, *i.e.* subjected to the same scattering properties.

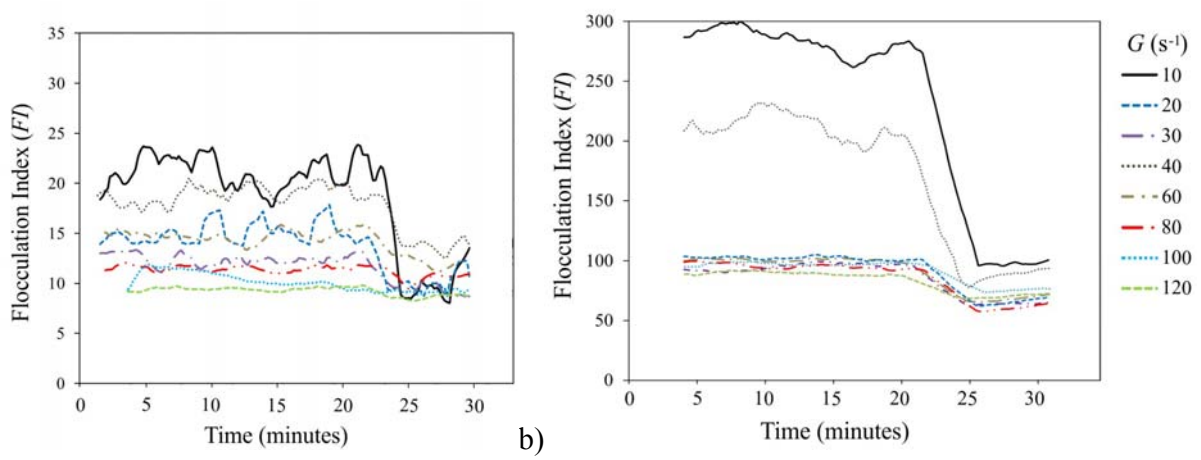

Figure 6. Time evolution of FI for different velocity gradients, *G* before and after induced breakage using 800 s^{-1} at time 25 minutes. (a) water type 1 for Al-Humic acid and (b) water type 2 for Al-Kaolin.

418

419 *3.3 Combined analyses of imagine and photometric dispersion methods*

420 Both analyses of image and photometric dispersion methods permitted to compare and correlate
421 data obtained from two different techniques *i.e.* intrusive and non-intrusive methods. Tables 1
422 and 2 present a comparison between the stable size and the floc strength for eight different
423 velocity gradients (G). The floc strength indicators presented are local stress (σ) and the force
424 factor (SF).

425 It is observed that, for each of the studied waters, SF, σ and d were strongly correlated with the
426 parameter G, resulting in Pearson correlation coefficient of 0.95, 0.99 and -0.89 for Al-Humic
427 and of 0.90, 0.99 and -0.80 for Al-Kaolin, respectively. Results found here corroborate well with
428 Li *et al.* (2007), who found that flocs formed at higher shear intensities have a small size and are
429 more resistant to breakage than those formed from lower ones. Floc resistance is determined by
430 both hydraulic shear rates and the strength of flocs bonds, which withstand shear forces during
431 floc formation (Jarvis *et al.*, 2005; Gregory, 2009). During floc formation in high shear rates, the
432 weak bonds might be broken, promoting a kind of selection, which results in floc fragments with
433 strong bonds. Therefore, with the higher shear rates, only the strongest bonds, which are more
434 likely to resist to the abrupt G variations, are maintained (Li *et al.*, 2007). This fact was shown by
435 the increase in SF value from 29.7% for G of 20 s^{-1} to 78.6% for G of 120 s^{-1} in water type 1 and
436 33.3% for G of 20 s^{-1} to 85.2% for G of 120 s^{-1} in water type 2.

437 Results in Tables 1 and 2 also suggested that the effect of G on SF might be more relevant for G
438 from 20 to 40 s^{-1}, and that d values can also decrease dramatically with the increase of G,
439 indicating there might be a limit above which floc strength is slightly affected by shear rate, but it
440 can strongly affect floc formation.

441 Results obtained from the two other strength indices used here seem to agree with the strength
442 coefficient (γ) analysis. The values of σ were nearly the same for water types 1 and 2, ranging
443 from 0.08 to 0.47 and from 0.07 to 0.44, respectively, with Pearson correlation coefficient (r)
444 between waters near to 1 (r = 0.97). These results are in agreement with previous work done by
445 Bache *et al.* (1999) who found Al-Humic flocs strength in the range of 0.08 to 0.42 N/m^2, and
446 close to the study by Li *et al.* (2007), who found Al-Kaolin flocs strength in the range of 0.01 to

447 0.24 N/m^2. Moreover, ANOVA test for σ variation with G indicates that floc strength is not
448 different between Al-Humic and Al-Kaolin for 0.05 of significance (p-value over 0.05), but it
449 depends on G and d only.

450 Regarding the strength factor (SF), results also have shown slight differences between aggregates
451 formed from Al-Humic and Al-Kaolin. Again, the ANOVA test for SF with G indicates that floc
452 strength is not different between Al-Humic and Al-Kaolin for 0.05 of significance, but it depends
453 on G and d only.

454 Despite the fact that the intrinsic characteristics of flocs formed from Al-Kaolin and Al-Humic,
455 namely, the scattering cross-section, altered FI measurements it seems that it did not affect floc
456 strength measurements by SF, as it is in agreement with the other two strength indicators.
457 Therefore, it is not expected that optical proprieties affect physical proprieties measurements,
458 such as resistance, and so the FI signal has been used by many researchers as an aggregation
459 indicator and as well as an indirect measurement of floc strength, *e.g.* Li *et al.* (2007), Yu *et al.*
460 (2010b and 2011), Su *et al.* (2017).
461

G (s^{-1})	SF (%)	σ N/m^2	d μm
20	36.73	0.07	337
30	56.82	0.11	287
40	55.56	0.12	200
50	69.70	0.20	245
60	69.34	0.23	217
80	83.33	0.29	173
100	83.33	0.36	157
120	95.00	0.44	146

Table 1. Shear rates (G), strength indexes (SF and σ) and stable size (d) for water type 1 (Al-Humic acid) during flocculation.

G (s^{-1})	SF (%)	σ N/m^2	d μm
20	33.33	0.08	407
30	35.56	0.09	236
40	61.82	0.17	298
50	65.42	0.16	197
60	58.00	0.24	228
80	62.00	0.36	217
100	78.00	0.39	167
120	85.23	0.47	154

Table 2. Shear rates (G), strength indexes (SF and σ) and stable size (d) for water type 2 (Al-Kaolin) during flocculation.

462 Figure 7 shows the relationship of the strength factor (SF), obtained from PDA, with the
463 parameter σ, which was calculated from image analysis data. It is observed that for both water

types, relatively high regression coefficients are obtained between *SF* and σ (R^2 of 0.92 and 0.76 for Al-Humic and Al-Kaolin, respectively) and a similar slope (close to 0.0070) is found for σ/*SF*. It is apparent that the values of both mentioned parameters enhance with increase in *G*, which are in agreement with results presented by Li *et al.* (2007) and Jarvis *et al.* (2005). Further, Pearson correlation coefficient between *SF* and σ resulted in 0.96 and in 0.87 for Al-Humic and Al-Kaolin, respectively. These strong correlations have confirmed that the macroscopic approach represented by *SF* is consistent with the theoretical method for different types of water, despite of the different methods used and the variations of *FI* signals.

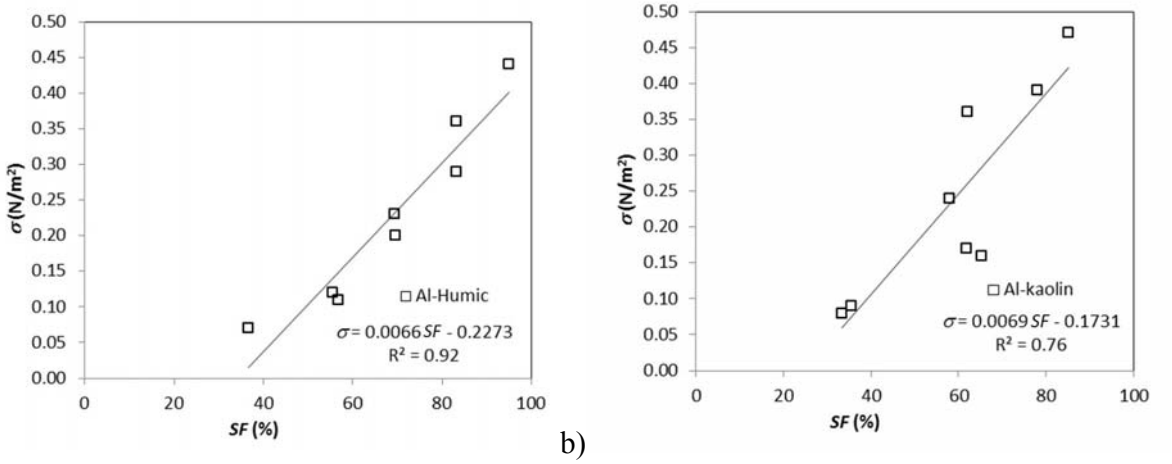

a) b)

Figure 7. Relationship between *SF* and σ for (a) water type 1 for Al-Humic acid and (b) water type 2 for Al-Kaolin.

Figure 8 shows the relationship between *SF* and *d*, *i.e.* the specific relationship between the strength force indicator obtained from PDA and values of average floc length, monitored by image analysis. The strength factor (*SF*) behaved nearly the same as *d* varied for Al-Humic and Al-Kaolin flocs, with smaller flocs resulting in higher resistant to *G* variations. These results are in agreement with the other strength indicator reported here (Table 1 and 2).

Moreover, despite of the differences between the two methods (PDA and image analysis), results indicate that the parameter *d*, derived from the non-intrusive image analysis, and *SF,* obtained from the *PDA* signal, behaved in similar way, with R^2 values near to 0.80 for Al-Humic and 0.60 for Al-Kaolin.

The lower R^2 value for Al-Kaolin is believed to be attributed to the different scattering area, as previously discussed. However, this does not explain why *SF* for Al-Humic and Al-Kaolin

493 behaved with no significant difference (p-value over 0.05), when exposed to rupture shear rate of
494 800 s^{-1}. A possible explanation is that flocs formed from sweep coagulation mechanism are
495 bigger than those formed from charge neutralization and their physical properties are likely
496 determined by coagulant only, as pointed out by Yu *et al.* (2015). Besides, floc characteristic size
497 was calculated based on the average of longest length, and so, it is expected that large flocs are
498 more prone to breakage by fragmentation when exposed to micro-scale dissipating eddies, thus
499 resulting in similar strength for Al-Humic and Al-Kaolin aggregates.

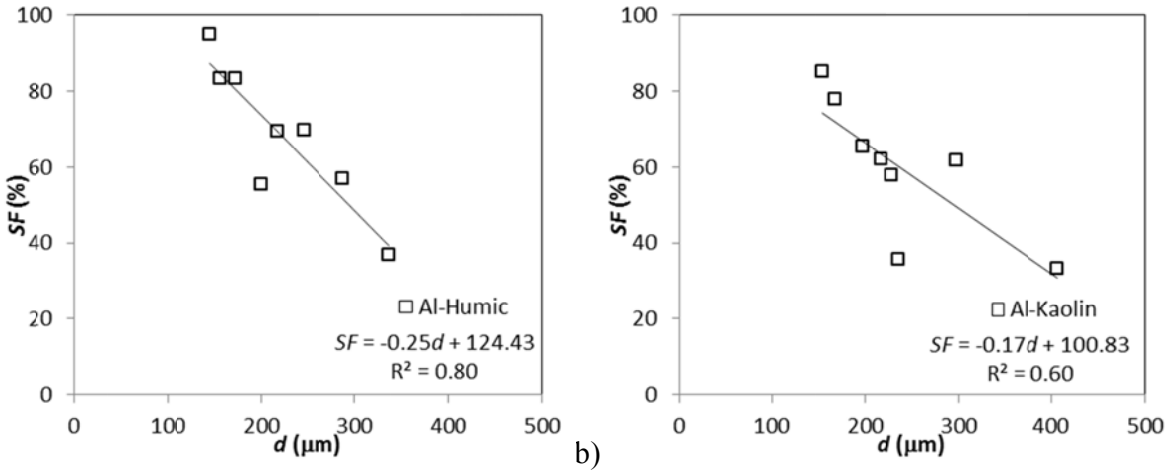

494 a) b)

496 Figure 8. Relationship between *SF* and *d*: (a) water type 1 – Al-Humic and (b) water type 2 – Al-
497 Kaolin.

497 **4. Conclusions**

405 Floc size and strength play an important role in separation processes used in water and
406 wastewater treatment, and the influence of different primary particles on the floc strength is still
407 poorly understood. The evidence that aggregates resistance is invariable with particles when
508 sweep coagulation is applied needs to be further investigated. Here, two aggregates formed by
509 Al-Humic and Al-Kaolin during flocculation were investigated using two techniques, namely
510 intrusive photometric dispersion analyser and non-intrusive image system. Both techniques were
511 applied to determine three floc strength indexes: the strength factors (*SF*), the local stress (σ) and
512 floc strength coefficient (γ). The main conclusions of this work are:

506

508 1. For Al-Humic and Al-Kaolin flocs, the strength factors (*SF*) and the local stress (σ) have
509 a positive variation in response to the increase of *G* because the high shear forces select

the strongest bonds within the aggregates. This means that higher *G* produces more resistant aggregates, however the size dependence for an individual separation process efficiency must be considered.

2. The comparison between the aggregates strength for Al-Humic acid and Al-Kaolin using floc strength coefficient (γ) indicates that both aggregates have nearly the same resistance, possible due to the precipitate hydroxide of alum mostly influencing floc size and strength. This finding reinforces the perspective that particles within a floc may have slight, or even no influence, on the floc strength when sweep coagulation is applied.
3. The intrusive photometric dispersion analyser and non-intrusive image-based system used in this study produced well correlated parameters, with a similar behaviour. However, the non-intrusive image method proved to be more reliable, as images are not influenced by the optical characteristics of the flocs.

Acknowledgements

Rodrigo B. Moruzzi is grateful to São Paulo Research Foundation (*Fundação de Amparo à Pesquisa do Estado de São Paulo*—FAPESP) Proc. 2017/19195-7 for financial support.

References

1. Bache, D.H. Floc rupture and turbulence: a framework for analysis. *Chem. Eng. Sci*. 59, 2521–2534. (2004). doi: http://dx.doi.org/10.1016%2Fj.ces.2004.01.055
2. Bache, D.H., Al-Ani, S.H. Development of a system for evaluating floc strength. *Water Sci. Technol.* 21, 529–537. (1989). doi: https://doi.org/10.2166/wst.1989.0255
3. Bache, D.H., Johnson, C., McGilligan, J.F., Rasool, E. A conceptual view of floc structure in the sweep floc domain. *Water Sci. Technol*. 36 (4), 49–56. (1997). doi: https://doi.org/10.1016/S0273-1223(97)00418-6
4. Bache, D.H., Rasool, E., Moffatt, D., McGilligan, F.J. On the strength and character of alumino-humic flocs. *Water Sci. Technol*. 40 (9), 81–88. (1999). doi: https://doi.org/10.1016/S0273-1223(99)00643-5
5. Bache, D.H., Rasool, E.R. Characteristics of alumina humic flocs in relation to DAF performance. *Water Sci. Technol*. 43 (8), 203–208. (2001). doi: https://doi.org/10.2166/wst.2001.0495

6. Biggs, C.A., Lant, P.A. Activated sludge flocculation: on-line determination of floc size and the effect of shear. Water Res. 34, 2542–2550. (2000).
7. Chakraborti, R. K.; Gardner, K. H.; Atkinson, J. F.; Van Benschoten, J. E. Changes in fractal dimension during aggregation. Water Research. v.37. p. 873–883. (2003).
8. Francois, R.J. Strength of aluminium hydroxide flocs. *Water Res*. 21, 1023–1030 (1987). doi: https://doi.org/10.1016/0043-1354(87)90023-6
9. Gregory and D.W. Nelson, A new optical method for flocculation monitoring. In Solid-Liquid Separation (J. Gregory, Ed.) Ellis Horwood, Chichester, pp 172-182. (1984).
10. Gregory, J. Monitoring particle aggregation process. Advances in Colloids and Interfaces v.147-148, 109-123. (2009). doi: https://doi.org/10.1016/j.cis.2008.09.003
11. Gregory, J. Optical monitoring of particle aggregates. *J. Environ. Sci.* 21, 2e7. (2009). doi: https://doi.org/10.1016/S1001-0742(09)60002-4
12. Gregory, J., Monitoring floc formation and breakage. In: Proceedings of the Nano and Micro Particles in Water and Wastewater Treatment Conference. International Water Association, Zurich September (2003)
13. Gregory, J., Nelson, D.W. Monitoring of aggregates in flowing suspension. Colloids Surf. 18, 175–188, (1986).
14. Jarvis P., Jefferson B., Gregory, J. and Parsons, S. A. A review of floc strength and breakage. *Water Res.* 39, 3121-3137. (2005). doi: http://dx.doi.org/10.1016/j.watres.2005.05.022
15. Li, T. Zhu, Z., Wang, D., Yao, C. and Tang, H. The strength and fractal dimension characteristics of alum–kaolin flocs. *International Journal Of Mineral Processing*, Beijing, Pr China, v. 82, n. 1, 23-29. (2007). doi: https://doi.org/10.1016/S0273-1223(99)00643-5
16. Leentvaar, J., Rebhun, M. Strength of ferric hydroxide flocs. *Water Res*. 17, 895–902. (1983).
17. Mikkelsen, L.H., Keiding, K. The shear sensitivity of activated sludge: an evaluation of the possibility for a standardised floc strength test. *Water Res*. 36, 2931–2940. (2002). doi: https://doi.org/10.1016/S0043-1354(01)00518-8
18. Mühle, K. Floc stability in laminar and turbulent flow. In: Dobias, B. (Ed.), Coagulation and Flocculation. Dekker, New York, pp. 355–390. (1993).

19. Oliveira, A.L. de, Moreno, P., Silva, P.A.G. da, Julio, M.D. and Moruzzi, R.B. Effects of the fractal structure and size distribution of flocs on the removal of particulate matter. *Desalination and Water Treatment.*, Vol. 57 (36). 1-12. (2015). doi: https://doi.org/10.1080/19443994.2015.1081833

20. Parker, D.S., Kaufman, W.J., Jenkins, D. Floc breakup in turbulent flocculation processes. *J. Sanit. Eng*. Div.: Proc. Am. Soc. Civ. Eng. SA1, 79–99. (1972). doi: https://pubs.acs.org/doi/abs/10.1021/la980763o

21. Moruzzi, R. B., Silva, P. A. G. Reversibility of Al-Kaolin and Al-Humic aggregates monitored by stable diameter and size distribution. *Brazilian Journal of Chemical Engineering.,* Vol. 35 (3). 1029-1038. (2018). doi: dx.doi.org/10.1590/0104-6632.20180353s20170098

22. Zhaoyang Su, Xing Li, Yanling Yang. Regrowth ability and coagulation behavior by second dose: Breakage during the initial flocculation phase. Colloids and Surfaces A 527, 109–114. (2017). doi: http://dx.doi.org/10.1016/j.colsurfa.2017.05.034

23. Wang, Y., Gao, B., Xu, X., Xua, W., Xub, G. Characterization of floc size, strength and structure in various aluminum coagulants treatment. Journal of Colloid and Interface Science v332, 354–359. (2009). doi: https://doi.org/10.1016/j.jcis.2009.01.002

24. Watanabe, Y., Flocculation and me. *Water Research*. (2017). doi: https://doi.org/10.1016/j.watres.2016.12.035

25. Yu, W., Gregory, J. and Campos, L. The effect of additional coagulant on the re-growth of alum–kaolin flocs. Separation and Purification Technology v74, 305–309. (2010a). doi: https://doi.org/10.1016/j.seppur.2010.06.020

26. Younker, J. M., Walsh, M. E. Effect of adsorbent addition on floc formation and clarification. *Water Research* 98. (2016). doi: https://doi.org/10.1016/j.watres.2016.03.044

27. Yu, W., Gregory, J. and Campos, L., Breakage and Regrowth of al Humic Flocs – Effect of additional Coagulant Dosage. Environ. Sci. Technol, no. 44. (2010b). doi: http://dx.doi.org/10.1021/es1007627

28. Yu, W., Gregory, J., Campos, L., Breakage and re-growth of flocs: Effect of additional doses of coagulant species. *Water Research,* 45. (2011). doi: https://doi.org/10.1016/j.watres.2011.10.016

599 29. Yu, W., Gregory, J., Campos, L., Graham, N. Dependence of floc properties on coagulant
600 type, dosing mode and nature of particles. *Water Research* 68, p 119-126. (2015). doi:
601 https://doi.org/10.1016/j.watres.2014.09.045
602 30. Yu, W., Hu, C., Liu, H., Qu, J. Effect of dosage strategy on Al-humic flocs growth and re-
603 growth. *Colloids and Surfaces A: Physicochem. Eng. Aspects*, 404, 106–111. (2012). doi:
604 https://doi.org/10.1016/j.colsurfa.2012.04.033
605 31. Yukselen, M. A. and Gregory, J. The reversibility of flocs breakage. *International Journal*
606 *of Mineral Processing*, v. 73, no. 2-4, p. 251-259. (2004). doi:
607 https://doi.org/10.1016/S0301-7516(03)00077-2
608 32. Yukselen, M.A. and Gregory, J. Breakage and reformation of alum flocs. *Environ. Eng.*
609 *Sci.* no. 19, p. 229–236. (2002). doi: https://doi.org/10.1089/109287502760271544
610 33. Zhong, R., Zhang, X., Xiao F., Li, X., Cai Z., Effects of humic acid on physical and
611 hydrodynamic properties of kaolin flocs by particle image velocimetry. *Water Research*
612 45. (2011). doi: https://doi.org/10.1016/j.watres.2011.05.006